Extension of the TAMSAT satellite-based rainfall monitoring over Africa and from 1983 to present

Article

Published Version

It is advisable to refer to the publisher's version if you intend to cite from the work. See Guidance on citing.

To link to this article DOI: http://dx.doi.org/10.1175/JAMC-D-14-0016.1

Publisher: American Meteorological Society

CentAUR

Central Archive at the University of Reading

Reading's research outputs online

Extension of the TAMSAT Satellite-Based Rainfall Monitoring over Africa and from 1983 to Present

ELENA TARNAVSKY, DAVID GRIMES,* ROSS MAIDMENT, EMILY BLACK,
RICHARD P. ALLAN, AND MARC STRINGER

Department of Meteorology, University of Reading, Reading, United Kingdom

ROBIN CHADWICK

Met Office Hadley Centre, Exeter, United Kingdom

FRANCOIS KAYITAKIRE

Institute for Environment and Sustainability, Joint Research Centre, Ispra, Italy

(Manuscript received 12 December 2013, in final form 21 August 2014)

ABSTRACT

Tropical Applications of Meteorology Using Satellite Data and Ground-Based Observations (TAMSAT) rainfall monitoring products have been extended to provide spatially contiguous rainfall estimates across Africa. This has been achieved through a new, climatology-based calibration, which varies in both space and time. As a result, cumulative estimates of rainfall are now issued at the end of each 10-day period (dekad) at 4-km spatial resolution with pan-African coverage. The utility of the products for decision making is improved by the routine provision of validation reports, for which the 10-day (dekadal) TAMSAT rainfall estimates are compared with independent gauge observations. This paper describes the methodology by which the TAMSAT method has been applied to generate the pan-African rainfall monitoring products. It is demonstrated through comparison with gauge measurements that the method provides skillful estimates, although with a systematic dry bias. This study illustrates TAMSAT's value as a complementary method of estimating rainfall through examples of successful operational application.

1. Introduction

Understanding the spatial and temporal variability of African rainfall is essential to agrometeorological applications such as drought monitoring and seasonal crop yield forecasting (Challinor et al. 2003; Teo 2006). In the absence of long-term ground observations of rainfall across Africa,

ⓐ Denotes Open Access content.

---

* We dedicate this paper to the legacy in African rainfall monitoring and its societal importance left by our coauthor and friend, Dr. David Grimes, who sadly passed away on 22 December 2011 and who a great many people sorely miss.

Corresponding author address: Elena Tarnavsky, Department of Meteorology, University of Reading, Earley Gate, P.O. Box 243, Reading RG6 6BB, United Kingdom.
E-mail: e.tarnavsky@reading.ac.uk

satellite-based rainfall estimates have provided a practical and complementary alternative. Here, we report on the extension of the Tropical Applications of Meteorology Using Satellite Data and Ground-Based Observations (TAMSAT) approach for rainfall estimation over Africa and from 1983 to present. As part of this, the 30-yr (1983–2012) TAMSAT African Rainfall Climatology and Time Series (TARCAT) dataset has been developed (Maidment et al. 2014). TARCAT benefits from the temporally consistent (climatology based) calibration described here and is updated in near–real time to constitute the TAMSAT rainfall estimates and derived products (see the appendix). These include rainfall estimates, 30-yr climatologies, and anomalies at dekadal (10 day), monthly, and seasonal time

steps, provided on a grid at spatial resolution of 0.0375° in latitude and longitude (approximately 4 km at nadir).

The TAMSAT method combines geostationary Meteosat data with gauge observations through a calibration approach that exploits both data sources. Until 2009, the TAMSAT approach had only been applied to northern and southern/eastern Africa during the respective rainy seasons May–October (Northern Hemisphere) and November–April (Southern Hemisphere), and the gauge data inputs had varied over time when calibrations were updated. The new pan-African calibration was undertaken to extend the spatial coverage of TAMSAT's rainfall estimates and derived products over the entire continent and the temporal extent of the time series from January 1983 to the present without varying the gauge data input.

TAMSAT rainfall estimates have been available since the early 1990s and have been validated for several regions and applications. Comparisons with other available products have been carried out, including for Kenya (Herman et al. 1997; Tucker and Sear 2001), West Africa (Laurent et al. 1998; Jobard et al. 2011; Snijders 1991), Ethiopia (Dinku et al. 2007), southern Africa (Thorne et al. 2001), and Uganda (Asadullah et al. 2008; Maidment et al. 2013). These showed that the TAMSAT approach outperforms or is comparable to other available satellite-based datasets with similar spatial and temporal resolution and extent. Other studies have focused on the factors that affect the accuracy of rainfall estimation (Milford et al. 1994; Dugdale et al. 1991; Grimes et al. 1999), demonstrating the utility of TAMSAT as a complementary approach for estimating rainfall in gauge-sparse regions.

Previous validations have used earlier versions of the TAMSAT data, calibrated against differing gauge inputs, which confirm the usefulness of the TAMSAT algorithm, but make it difficult to assess the reliability of rainfall estimates over time. Furthermore, these studies covered only selected regions in Africa and focused mainly on the rainy seasons. Hence, from a users' perspective, previously there has been a lack of information on the reliability of the TAMSAT (as well as other) rainfall estimates in various African regions. For TAMSAT to be useful for decision making, it is essential that the reliability of the data is understood. Operationally, we address this need through the establishment of a system for validation of dekadal TAMSAT rainfall estimates in near–real time against independent rain gauge observations.

Hence, this study reports on (i) the spatially contiguous and temporally consistent calibration applied to the quality-controlled archive of Meteosat thermal infrared (TIR) data, and (ii) the systematic approach for routine, near-real-time validation of the operational dekadal

rainfall estimates. Results are discussed in the context of the use of TAMSAT rainfall estimates by those most in need of timely information on rainfall at organizations concerned with agrometeorological monitoring and forecasting. In the final part of the paper, we reflect on the range of rainfall products and the complementary role of TAMSAT's pan-African rainfall monitoring.

2. Data and methods

There are three aspects to the TAMSAT system. The first is the calibration of the algorithm, using a newly compiled archive of rain gauge observations and contemporaneous cold cloud duration (CCD) fields. The calibration is carried out for 1983–2010. The second aspect is the provision of near-real-time rainfall estimates, derived by applying the calibration to the CCD generated from Meteosat imagery transmitted in real time. Finally, outside the calibration period (i.e., from 2011 onward), gauge data are used to independently validate dekadal TAMSAT rainfall estimates.

TAMSAT's use of a climatology-based calibration over 28 years (1983–2010), based on the relationship between CCD and gauge data, means that trends and anomalies inferred from TAMSAT data are not biased by changes in gauge coverage (see section 2a and Fig. 3, described below). This is particularly important for regions with sparse gauge networks, regions where there has been substantial data loss, and in regions characterized by steep gradients of rainfall that may not be captured by sparse gauge networks. It should also be noted that independent validation is only possible as TAMSAT rainfall estimates are not merged with gauge observations. Moreover, the validation metrics provide useful input into decisions based either solely on TAMSAT data (in regions with no gauges) or on analysis of TAMSAT, model output, and gauge observations (Kucera et al. 2013; Boyd et al. 2013).

In the rest of this section, we first summarize the three data sources used in the TAMSAT system: Meteosat imagery, the historical gauge archive, and the real-time gauge validation data (section 2a). The following section (section 2b) outlines the methodology for calibrating TAMSAT and extending the algorithm throughout Africa. We then describe the methodology for validating the dekadal TAMSAT rainfall estimates in real time and how we have exploited these validations to comment on the skill of the TAMSAT approach.

a. Data

1) METEOSAT THERMAL INFRARED IMAGERY

The TAMSAT rainfall estimation approach is based on TIR imagery acquired every 30 min until June 2006

and every 15 min from July 2006 onward. The high-frequency sampling captures short-duration rain events that provide much of the seasonal rainfall in parts of the African continent such as the Sahel. For example, squall lines characteristic of the West African Sahel deliver over half of the precipitation in the first 30 min of the squall line passage, which typically lasts 2–4 h (Milford and Dugdale 1984). Hence, the high-frequency TIR imagery allows TAMSAT to sample at the time and space scale of individual storms, improving its representation of the temporal and spatial variation in rainfall, including the contribution of short-duration events. Although the long-term Meteosat TIR record consists of data acquired by instruments on the Meteosat First Generation (*Meteosat-2–7*) and Meteosat Second Generation (*Meteosat-8–10*) platforms, the calibration information supplied by the European Organisation for the Exploitation of Meteorological Satellites (EUMETSAT) yields a stable TIR record adequate for generating rainfall estimates. Moreover, the TAMSAT algorithm was found to be insensitive to small changes in cloud-top temperature because of the use of Meteosat radiances from different satellite instruments in rainfall estimation (Maidment et al. 2014).

2) RAIN GAUGE DATA ARCHIVE FOR CALIBRATION OF THE TAMSAT RAINFALL ESTIMATION ALGORITHM, 1983–2010

Previous versions of the TAMSAT rainfall estimates were based on temporally varying calibrations derived only for the main rainy season months in northern (May–October) and southern/eastern (November–April) Africa using varying subsets of local gauge data from the 1986–2000 time period. Over regions such as the Sahel and eastern and southern Africa, these local gauge datasets were obtained in a series of workshops conducted in cooperation with African national meteorological agencies (NMAs) since the early 1980s. These datasets are not necessarily reported on the Global Telecommunication System (GTS) network of the World Meteorological Organization (WMO).

Data from local, proprietary gauge archives were first subjected to quality control when used by NMA staff in African countries for calibrating the TAMSAT algorithm in a series of local and regional workshops. For the purposes here, the TAMSAT gauge archive was expanded to include data over Africa for all months and over a time period that overlaps with the quality controlled TIR image archive from January 1983 to December 2010, from which contemporaneous dekadal CCD fields were derived. As new gauge datasets from multiple sources were added to the existing TAMSAT archive, duplicate records were eliminated and dekadal sequences with fewer than 10 days

of precipitation reporting have been excluded. The data records that passed the above tests were ingested into the new TAMSAT gauge archive. The archive contains nearly 350 000 dekadal gauge records in total from approximately 4300 locations, which were used in the climatology-based calibrations. Figure 1 shows the total density of gauges in the newly compiled archive on a 1° × 1° latitude–longitude grid over the 1983–2010 time period.

A summary of the number of wet and dry dekads in the gauge archive is presented in Fig. 2 by month for the first decade (1983–92), second decade (1993–2002), and the remaining 8 years in the archive (2003–10). Figure 2a highlights that during 1983–92 the gauge archive consists mainly of data for May–October (the rainy season in the Sahel region). This is due to data that were made available for rainy season calibrations through a series of field workshops carried out by TAMSAT in the 1980s and 1990s. In the second decade (1993–2002), the archive is the most complete for all months from the three time periods under consideration (Fig. 2b). This is due to the regular contribution of gauge data from WMO's GTS network from 1993 to present, as these were recently made available to TAMSAT by the European Commission (EC)'s Joint Research Centre (JRC) in the framework of a service contract to improve rainfall estimation for food security monitoring and early warning in Africa. Figure 2 shows that, overall, between 11 300 and 26 200 (approximately 59% and 79%, respectively) of station dekads were wet across Africa for any given month. It is worth noting that the calibrations represent a 1983–2010 climatological average, and the majority of the gauge observations originated from the 1993–2002 time period (Fig. 2).

Figure 3a shows the number of gauges used in the TAMSAT pan-African calibration. It is evident that substantially more gauge records are used in a climatology-based calibration (varying monthly but not interannually) than are available for any given month. Figure 3b illustrates the varying number of gauges over time that are used in a method such as the Global Precipitation Climatology Project (GPCP) dataset (Huffman et al. 1997; Adler et al. 2003), which relies mainly on gauge data from the Global Precipitation Climatology Centre (GPCC). It is furthermore clear from Fig. 3b that there has been a substantial loss of gauge data during the last decades in the GPCC records over the past three decades.

3) NEAR-REAL-TIME RAIN GAUGE DATA FOR OPERATIONAL VALIDATION OF THE TAMSAT DEKADAL RAINFALL ESTIMATES, 2011–PRESENT

Data from the weather stations that are part of WMO's GTS network were used to develop a new system for operational validation of the 10-day TAMSAT rainfall estimates. Independent dekadal gauge observations
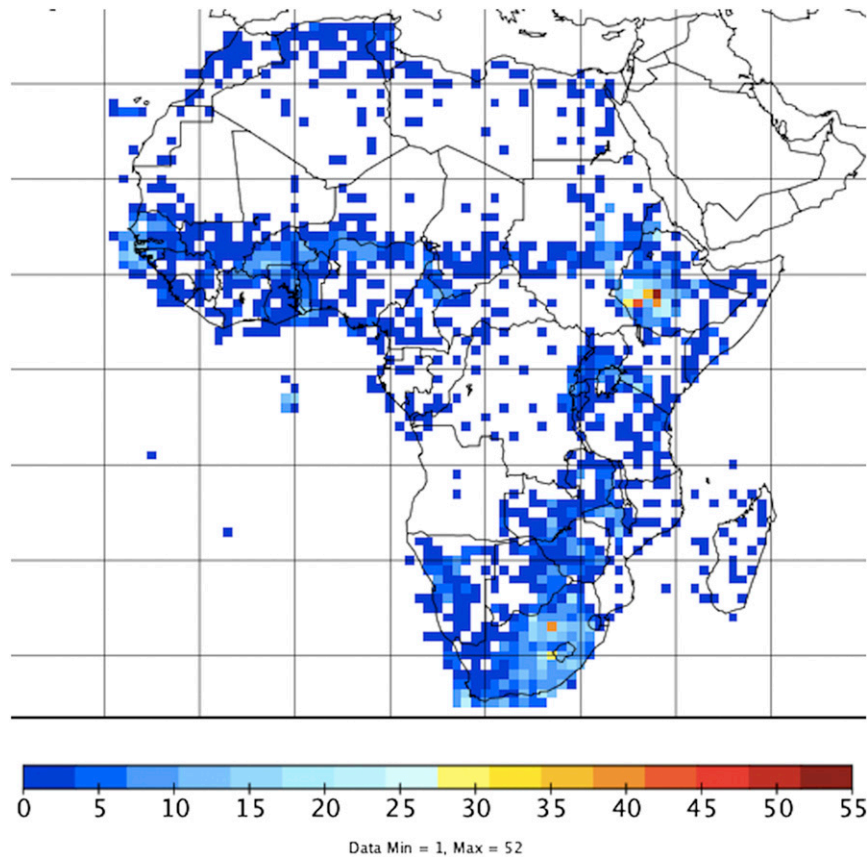
FIG. 1. Number of rain gauges in the TAMSAT archive per $1° \times 1°$ latitude–longitude grid. Note that although rainfall observations from islands (other than Madagascar and the Canary Islands) are part of the gauge data archive, TAMSAT does not estimate rainfall in these places.

were compiled from quality-checked daily synoptic reports with a maximum of 1-day latency after the end of a given dekad and are made available to TAMSAT for operational validation in near–real time. Only data from January 2011 to present are included in the validation as the data up to December 2010 were used in the calibration. The near-real-time data are used to produce monthly validation reports for internal evaluation and for distribution to the user community from the website of TAMSAT (www.met.reading.ac.uk/~tamsat). Generally, about 20%–25% of over a thousand stations report each dekad, rendering any effort for a comprehensive validation less complete than might be desirable from a user perspective.

b. Methods

1) TEMPORALLY CONSISTENT CALIBRATION FOR DEKADAL RAINFALL ESTIMATION

TAMSAT uses the CCD method of rainfall estimation, which assumes predominantly convective rainfall

and a positive linear relationship between the lengths of time convective clouds are present (CCD hours) and the amount of rainfall at the surface (Grimes et al. 1999; Richards and Arkin 1981). The scientific basis of the TAMSAT CCD-based approach for near-real-time rainfall estimation at dekadal (10 day) scale through local calibrations has not been modified since originally proposed (Grimes et al. 1999; Milford and Dugdale 1984). This methodology is summarized below.

The CCD method is based on the principle that deep convective clouds are likely to deliver the most rainfall. Observational findings, moreover, have demonstrated a close relationship between CCD from TIR imagery and the presence of rainfall, especially pronounced in tropical areas (Arkin 1979; Richards and Arkin 1981). Dekadal CCD fields are derived at $-30°$, $-40°$, $-50°$, and $-60°C$ (corresponding to approximately 243, 233, 223, and 213 K, respectively), as these have been shown to discriminate well between rain and no-rain areas. For each month a set of contingency tables (one for each temperature threshold T) are evaluated to select the

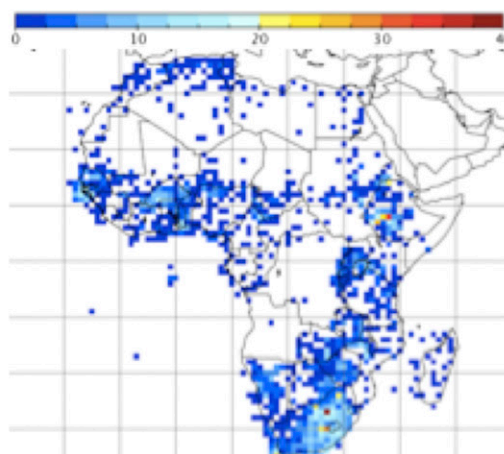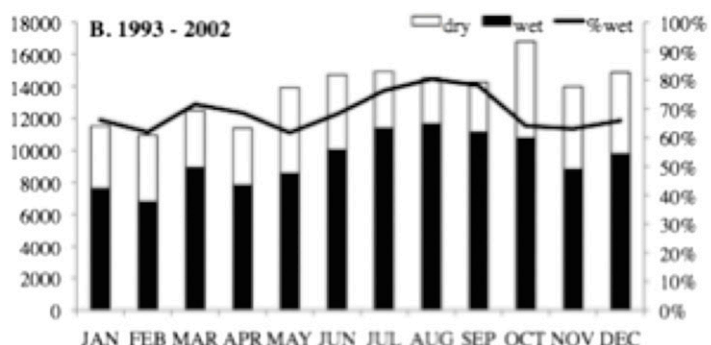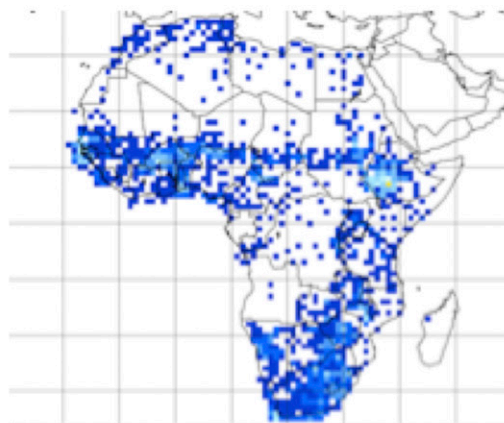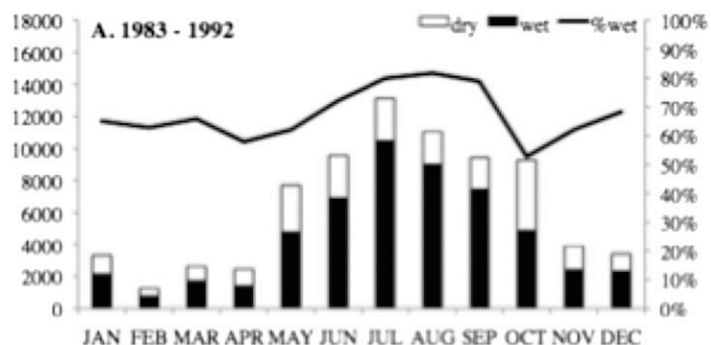FIG. 2. Summary of dry (rainfall = 0 mm) and wet (rainfall > 0 mm) dekadal (10 day) rain gauge observations used for calibration of the TAMSAT rainfall estimation algorithm and respective maps of gauge densities plotted on a 1° × 1° latitude–longitude grid for (a) 1983–92, (b) 1993–2002, and (c) 2003–10.
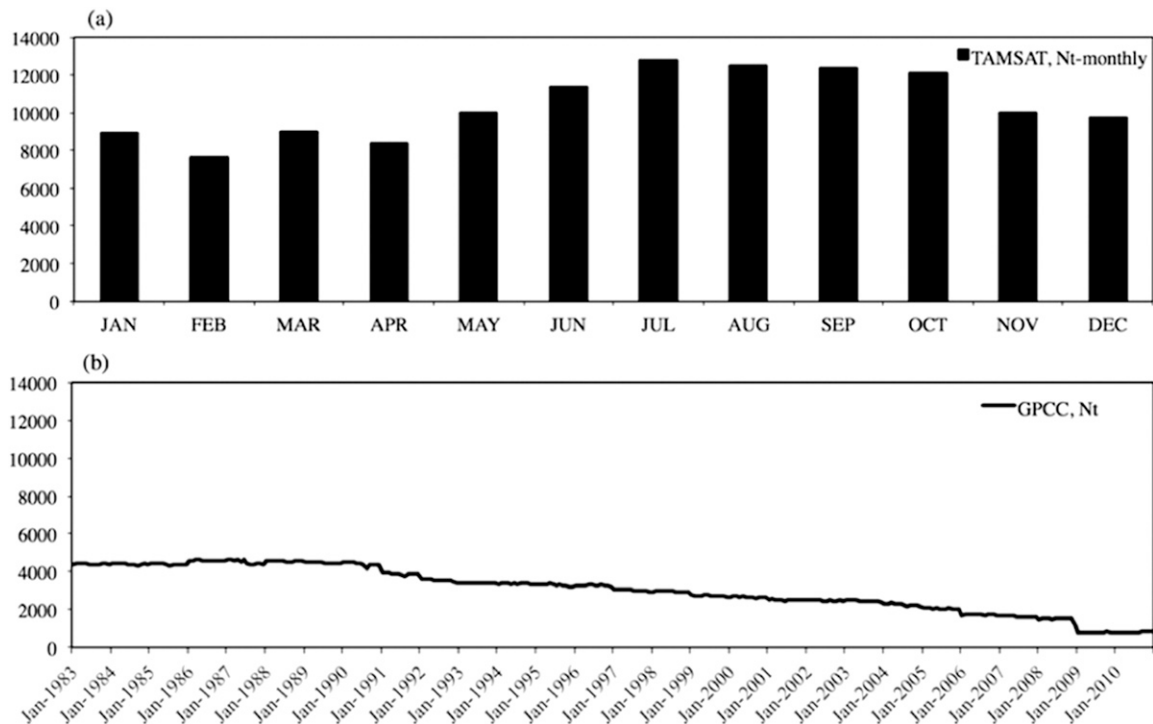
FIG. 3. Total number of gauges Nt (a) used in the TAMSAT climatology-based calibration (varying monthly but not interannually) and (b) in the GPCC archive (varying over time and exhibiting a nearly fourfold reduction from 1983 to 2010).

optimal regression function, that is, one that shows the highest level of agreement with the gauge data as to rainfall occurrence (Grimes et al. 1999). The optimum T is selected where the number of occasions on which the satellite and gauge agree is much greater than the number of disagreements ($n_{11} + n_{22} \gg n_{12} + n_{21}$) and the number of occasions for which gauges register rain but CCD is zero is roughly balanced by the number of occasions for which the gauge registers no rain but there is some CCD ($n_{12} \cong n_{21}$; see Table 1). If the contingency tables point to different optimum T, then the first condition is prioritized to select the threshold, at which the agreement between gauge and satellite is maximized.

Once the optimum T is established for each month and calibration region, suitable calibration parameters (slope a_1 and intercept a_0) are derived as follows:

$$R = \begin{cases} a_0 + a_1 \times \text{CCD} & \text{CCD} > 0 \\ 0 & \text{CCD} = 0 \end{cases}, \qquad (1)$$

where R is the median of gauge-observed dekadal rainfall in millimeters, and CCD is the midpoint of the CCD bin in hours at the optimum T. It has been shown that brightness temperature from TIR imagery in approaches such as the Geostationary Operational Environmental Satellite (GOES) precipitation index (GPI) (Arkin and Meisner 1987) is not suitable for capturing the effect of warm rain (Behrangi et al. 2009; Dybkjær 2003). Thus, the TAMSAT approach uses an intercept term to account for the warm-rain effect (Dybkjær 2003). A linear relationship is assumed between dekadal CCD hours and rainfall total. More sophisticated statistical methods such as multiple regression and logarithmic regression have shown insignificant improvement over simple linear regression (Milford et al. 1994). The method for determining the calibrations optimizes the estimation of the median rather than the mean rainfall event as relevant for drought detection and monitoring applications. This is because unlike the mean, the median is not susceptible to rare extremes. Additionally, rainfall has a nonnormal and skewed distribution, for which the median captures the location better than the mean. The optimum T and calibration parameters

TABLE 1. Contingency table for determining optimal threshold temperature from the relationship between collocated dekadal (10 day) CCD (h) and rainfall observations at gauge locations G (mm).

	CCD = 0	CCD > 0
Rainfall$_G$ = 0	n_{11}	n_{12}
Rainfall$_G$ > 0	n_{21}	n_{22}

vary spatially (across calibration regions) and temporally (across months).

2) EXTENDING THE TAMSAT APPROACH OVER AFRICA

Extending the TAMSAT approach over Africa through climatology-based calibrations requires information on the relationship between cold cloud duration inferred from the TIR imagery and rainfall observed on the ground throughout the continent. However, because of the complexities of convective rainfall, both the temperature threshold and the linear regression relationship depend on the local characteristics of the area under consideration (Todd et al. 1995, 1999). This makes such empirical approaches applicable to the space–time domain, for which they have been derived (Richards and Arkin 1981). The statistical relationship between CCD and ground-based rainfall observations might be extended to other areas and times depending on the similarity of meteorological conditions. Results from a calibration of the CCD algorithm over the Sahel region using a latitude-dependent correction to account for the varying climatic conditions caused by the movements of the intertropical convergence zone (ITCZ) demonstrated that the use of constant calibration zones in the Sudan–Sahel region is inadequate (Dybkjær 2003). Additionally, Chadwick et al. (2010) showed that using a single calibration over West Africa is inappropriate even for a multispectral satellite rainfall estimation product, as the relationship between satellite-observed radiances and rainfall varies substantially over the region.

To accommodate the variability of the African climate, the continent was split into 25–30 calibration subregions for each month, taking into account zones defined through several TAMSAT-led calibration workshops carried out in the 1980s and 1990s. The calibration region boundaries vary monthly, reflecting the movement of the ITCZ as well as regional topography and distance to the coast, ensuring that every climatologically homogeneous region is covered in every month by sufficient gauge data for a statistically reliable calibration. Figure 4 shows an example of the calibration region boundaries for May.

The uneven distribution of gauges across Africa has implications for defining climatologically meaningful calibration zones. It was determined that approximately 30–40 gauges (or at least 100 gauge–CCD data pairs) are required for reliable calibration, although this criteria for data sufficiency depends on the area and local characteristics of the calibration region (Milford et al. 1994; Thorne et al. 2001). For example, in countries such as Angola, South Sudan, Democratic

Republic (DR) of the Congo, Madagascar, as well as most countries above 20°N, the gauge coverage is far from optimal and calibration parameters are inferred from an enlarged calibration region that includes areas with gauge observations. Since we use a 28-yr-long gauge archive, reasonable calibrations were obtained in many instances even in areas of sparser gauge network coverage.

The use of calibration zones inevitably introduces spatial discontinuities into the TAMSAT rainfall estimates that tend to be most accentuated in long-term monthly climatologies and less so in operational dekadal and seasonal products. Hence, as a final step, before applying the calibrations to derive rainfall estimates, smoothing by spatial averaging is applied to the optimum T, slope, and intercept values along the borders of calibration regions to avoid sharp discontinuities and to account for the transition between meteorological zones (Milford et al. 1994). A large smoothing filter ($\sim 1.0°$) is used in most regions and a smaller filter ($\sim 0.5°$) is used for calibration regions that are narrower than 2° in latitude or longitude directions. The final set of optimum T, slope, and intercept parameters is applied to the TIR archive data to generate the 30-yr TARCAT dataset and in near–real time to build up a consistent time series of rainfall estimates and derived products. Although this still can leave some visual lines along boundaries of some calibration regions for some months, it makes best use of data from sparsely distributed gauge networks across Africa. More importantly, the extended coverage of the TAMSAT rainfall monitoring products allows for pan-African analysis of rainfall and drought conditions in near–real time and for the evaluation of dryness and wetness signals relative to a temporally consistent, long-term record—a feature that is not available for products that blend in gauge data.

3) OPERATIONAL VALIDATION OF DEKADAL RAINFALL ESTIMATES

The purpose of the operational validation is to enhance the usefulness of the dekadal TAMSAT rainfall estimates through direct comparisons with independent gauge observations in near–real time. The near-real-time validation presented here is a useful indication of algorithm performance across Africa and relative to independent gauge observations from January 2011 to present.

Validation reports are compiled shortly after the end of each month for the three dekads of that month and disseminated via the TAMSAT website. The sparse GTS network and the varying number of reporting gauges in each dekad across the continent [see section 2a(3)] do not
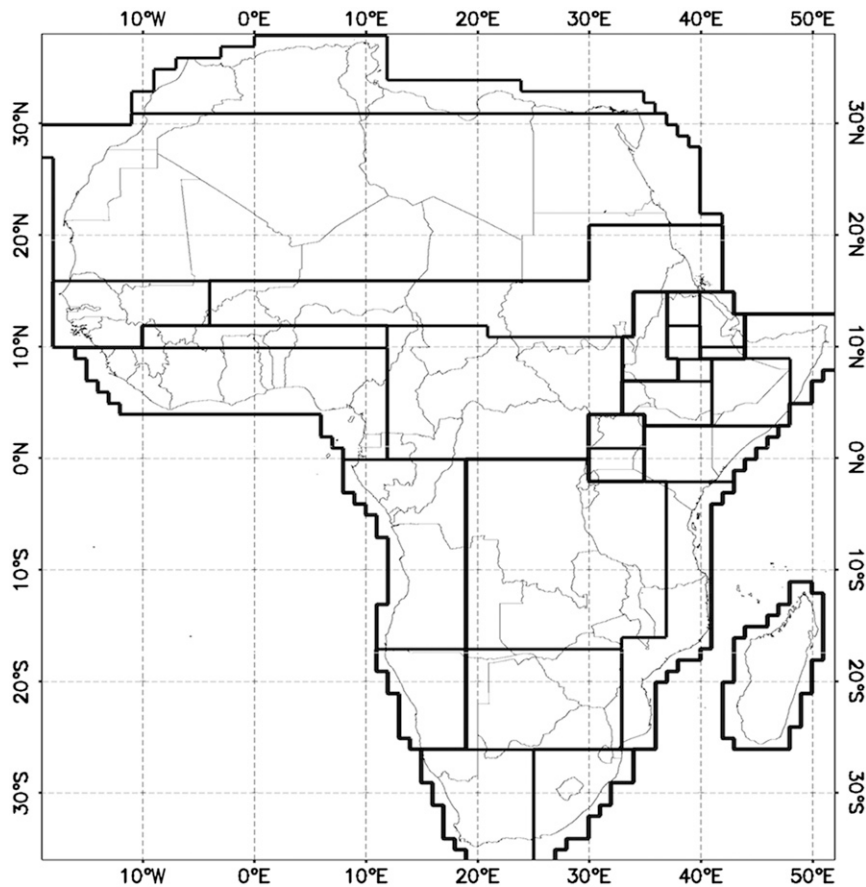
FIG. 4. Example map of TAMSAT pan-African calibration regions for May.

allow for robust implementation of spatial interpolation methods such as geostatistical kriging or local validation reports over small regions. Hence, the operational validation is based on pixel-to-point comparison of satellite-based rainfall estimates against ground-based rainfall observation, and statistics are spatially averaged across Africa. As gauges measure rainfall at a point and satellite-based rainfall estimates represent an areal average, it is to be expected that satellite-based rainfall estimates will differ from rainfall observed on the ground at gauges. Despite the best efforts at quality control, some gauges will still be inaccurate, and despite careful algorithm calibration, rainfall estimates (indirectly inferred from satellite data) will still be imperfect. Agreement in absolute terms is not to be expected; the validation is a useful indication of the difference between the rainfall observed at a point in space and that estimated over satellite pixels.

The validation reports include a combination of binary (dichotomous) and summary statistics (Table 2) that quantify relative and absolute differences between rainfall estimates and observations and include a set of exploratory plots (maps and scatterplots). The binary statistics are based on contingency tables constructed for each dekad's satellite-based estimate and collocated gauge observation of rainfall. These include the probability of detection (POD), false-alarm ratio (FAR), ratio bias (BIAS), and three commonly used skill scores: the Heidke skill score (HSS), Hanssen–Kuipers skill score (HKSS), and equitable threat score (ETS). The summary statistics for each dekad are calculated for point–pixel collocated pairs, for which rainfall above $1 \, \text{mm dekad}^{-1}$ was detected (category D in Table 2). These include regression coefficients (slope and offset), Pearson correlation, bias (additive bias or mean error) calculated as the mean difference between the TAMSAT estimate and the gauge observation across Africa, and percent bias calculated relative to gauge values. Additionally, for each dekad, we calculate the root-mean-square deviation (RMSD) and normalize the RMSD by the range of gauge observations to produce the normalized RMSD (NRMSD).

For the comparison of satellite-based estimates and gauge observations in absolute terms, bands of dekadal

TABLE 2. Summary of validation statistics. Here, S is the satellite-based rainfall estimate, G is the gauge-based rainfall observation, N is the number of gauge locations, i is the location index, and σ is the standard deviation. Variables A–D form a contingency table: For $G <$ 1 mm dekad^{-1}, A corresponds to $S < 1$ mm dekad^{-1} and B corresponds to $S \geq 1$ mm dekad^{-1}; for $G \geq 1$ mm dekad^{-1}, C corresponds to $S < 1$ mm dekad^{-1} and D corresponds to $S \geq 1$ mm dekad^{-1}.

	Equation	Range	Interpretation
Dichotomous statistics			
POD	$\dfrac{D}{C+D}$	$[0, 1]$	1: perfect
FAR	$\dfrac{B}{B+D}$	$[0, 1]$	0: no false detection
BIAS	$\dfrac{B+D}{C+D}$	$[0, +\infty)$	1: perfect <1: underforecast >1: overforecast
HSS	$\dfrac{2(AD - BC)}{(A+B)(B+D)+(C+D)(A+C)}$	$(-\infty, 1]$	1: perfect 0: no skill
HKSS	$\dfrac{AD - BC}{(A+B)(C+D)}$	$[-1, 1]$	1: perfect 0: no skill
ETS	$\dfrac{D - D_R}{B+C+D-D_R}$, where $D_R = \dfrac{(C+D)(B+D)}{A+B+C+D}$	$[-1/3, 1]$	<0: no skill
Summary statistics			
Pearson correlation $(-)$	$\dfrac{1}{N-1} \sum\limits_{i=1}^{N} \left(\dfrac{S_i - \overline{S}}{\sigma_S}\right)\left(\dfrac{G_i - \overline{G}}{\sigma_G}\right)$	$[-1, 1]$	
(Additive) bias (mm dekad^{-1})	$\dfrac{1}{N} \sum\limits_{i=1}^{N} (S_i - G_i)$	$(-\infty, +\infty)$	
Percent bias (%)	$\dfrac{\sum\limits_{i=1}^{N} (S_i - G_i)}{\sum\limits_{i=1}^{N} G_i} \times 100$	$(-\infty, +\infty)$	
RMSD, RMSD > 0 (mm dekad^{-1})	$\sqrt{\dfrac{1}{N} \sum\limits_{i=1}^{N} (S_i - G_i)^2}$	$[0, +\infty)$	
NRMSD, NRMSD > 0 (%)	$\dfrac{\text{RMSD}}{G_{\max} - G_{\min}} \times 100$	$[0, +\infty)$	

rainfall totals are not to be narrower than 10–20-mm rainfall because this is the accuracy with which gauges provide estimates of the average rainfall over a pixel (Milford et al. 1994). Thus, for visualizing absolute differences in the maps and scatterplots of the bias, we have selected the following ranges of dekadal rainfall totals: below −100-mm, from −100- to −50-mm, from −50- to −10-mm, from −10- to 10-mm, from 10- to 50-mm, from 50- to 100-mm, and above 100-mm difference. As differences are calculated for the TAMSAT rainfall estimate S minus the gauge observation G (Table 2), negative values indicate relative underestimation and positive values indicate relative overestimation of rainfall by TAMSAT. Although differences between point and pixel rainfall over larger 10-day totals decline substantially and are very much dependent on the particular storm characteristics, these are shown to be as much as

35% (12.5 in 36 mm) in a case study in Niger (Flitcroft et al. 1989). The −10- to 10-mm difference thus represents the difference expected from the point-to-area comparison, although this can be much higher depending on the frequency distributions of particular storms (Flitcroft et al. 1989).

The statistics compiled during the validation process are also collated over time to give an indication of how well the TAMSAT method performs when applied continent-wide. The results of this analysis are described in the next section.

3. Results

For the first time, TAMSAT has generated pan-African, temporally consistent time series of dekadal rainfall estimates and derived products and compared
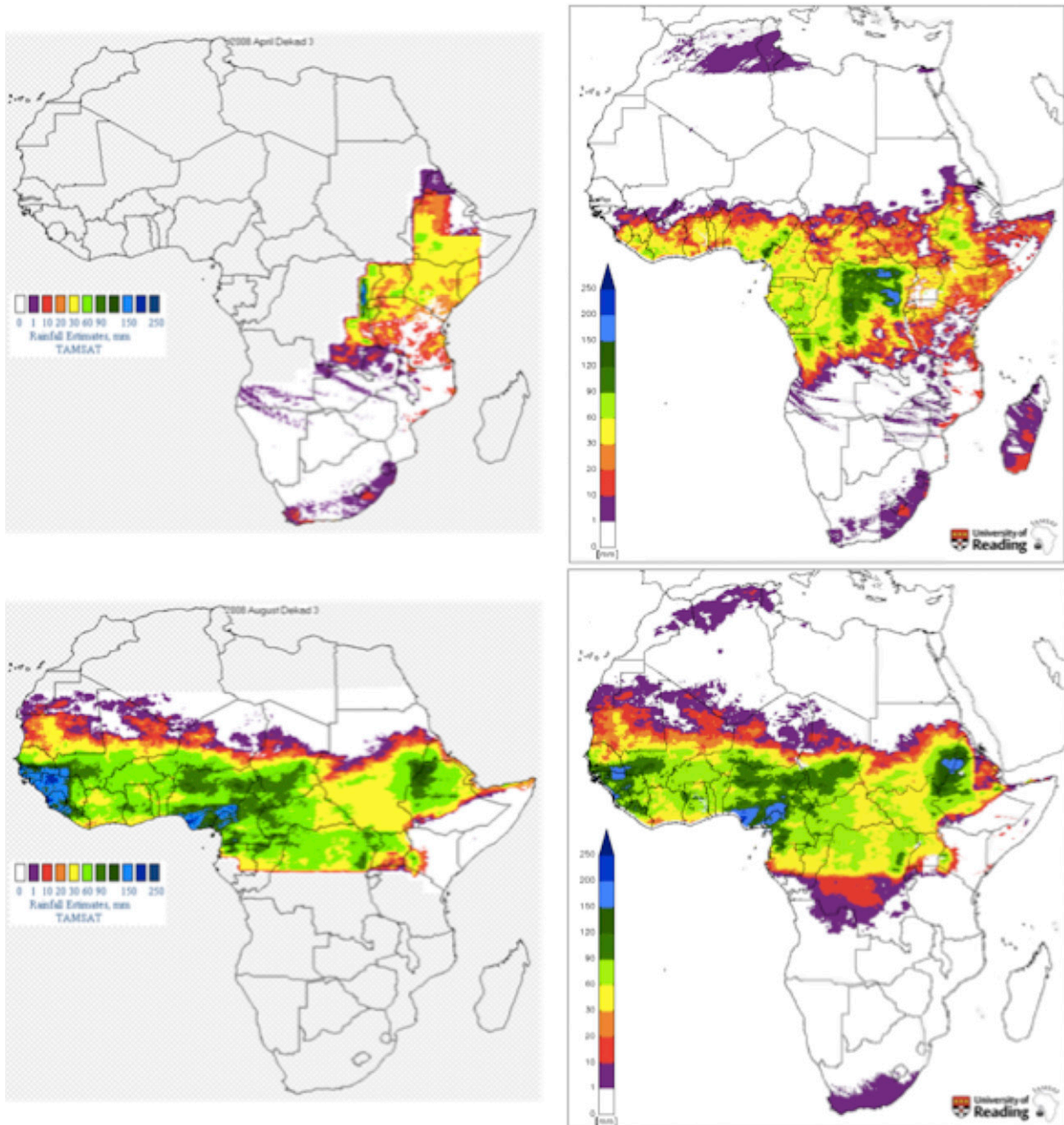
FIG. 5. Example of dekadal (10 day) TAMSAT rainfall estimates for dekad 3 for (top) April and (bottom) August of 2008 based on the (left) old (rainy season only, regional) and (right) new (all season, spatially contiguous) calibrations.

these against independent gauge observations in near–real time. Figure 5 shows examples of the extended spatial coverage of the dekadal rainfall estimates for the dekads 3 of April and August 2008 from the old (rainy season, regional) and the new (all season, spatially contiguous) calibrations. The new quick-look images used as an example here are plotted using the same color scheme as the old images for comparison. It is worth

noting that the spatial patterns of rainfall are very similar over the areas that overlap. The algorithm based on local calibrations can result in spatial discontinuities along the boundaries of some calibration regions in some months especially where very few gauge data are available (e.g., DR Congo, top-right panel in Fig. 5), but that spatial continuity is improved over regions with good data coverage (e.g., West African Sahel, bottom-left
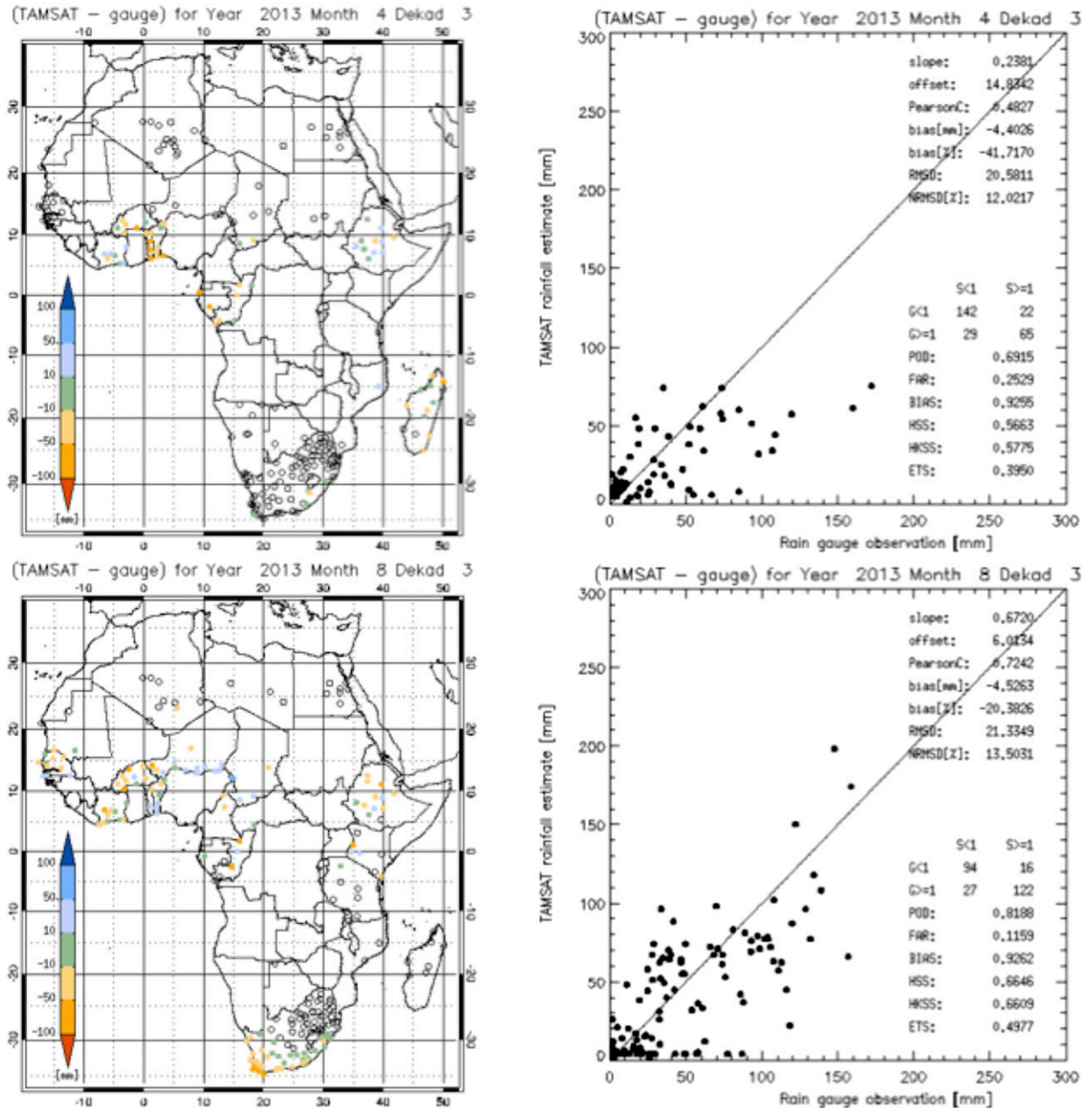
FIG. 6. Example validation maps and scatterplots showing absolute differences between dekadal (10 day) TAMSAT rainfall estimates and rain gauge observations for dekad 3 of (top) April and (bottom) August of 2013. Blue circles show where TAMSAT is higher and orange circles show where TAMSAT is lower than the gauge observation; open circles indicate no rainfall.

panel in Fig. 5). As would be expected, in regions where warm rain persists, TAMSAT will tend to underestimate rainfall, or it will miss warm rain completely, if CCD is 0 h [Eq. (1)]. However, within a given calibration zone, this would happen on extreme occasions at the 10-day temporal aggregation scale, considering that many pairs of gauge–CCD data are analyzed to derive the rainfall estimates.

Figure 6 presents an example of validation maps and plots of absolute differences between satellite-based estimates and corresponding gauge observations of rainfall for dekad 3 of April and August 2013. The contingency tables (see scatterplots in Fig. 6) show that TAMSAT generally agrees with gauge observations in the detection of wet dekads (rainfall > 1 mm dekad^{-1}) with POD of approximately 0.69 and 0.82, and a low

FAR of approximately 0.25 and 0.12 for April and August, respectively. The BIAS is above 0.92 for both April and August, and the HSS, HKSS, and ETS show good skill of TAMSAT with score values slightly higher for August than for April in this example (Fig. 6).

Although summary statistics are computed as spatial averages, for locations identified as wet in both TAMSAT estimates and gauge observations ($N = 65$ in April and $N = 122$ in August), the bias is relatively low (~ -4 mm dekad^{-1}), RMSD is within the error boundaries of gauge observations (~ 21 mm dekad^{-1} for April and August), and NRMSD is approximately 12% and 13% for April and August, respectively (Fig. 6). According to the scatterplots presented in Fig. 6, TAMSAT tends to underestimate rainfall above 70–100 mm dekad^{-1}. This partially relates to the optimizing of TAMSAT calibrations for detecting the median rainfall event, whereas point-to-pixel validation effectively compares rainfall estimates against mean gauge observations. Although the point-to-pixel validation method used here introduces a dry bias, which is representative of the point-to-pixel mismatch in estimating rainfall over an area, using the median is more appropriate than the mean for deriving area-averaged rainfall estimates (Flitcroft et al. 1989). Figure 6 highlights that TAMSAT has skill outside the main rainy season over parts of southern Africa in both April and August, which is important because in some African regions there can be a secondary rainy season and/or rain events during the dry season that are crucial for crop growth. Thus, skill outside the main rainy season provides valuable information.

Figure 7a shows the Pearson correlation coefficient collated over time for the dekads under consideration here from January 2011 to December 2013 ($N = 108$ dekads) where gauge and satellite detected a wet dekad. Although calculated as a spatial average across Africa and over the entire time period considered (i.e., including dry and rainy seasons), the mean Pearson correlation is approximately 0.6 (black dashed line, Fig. 7a), which shows a moderate positive relationship with ground-based rainfall observations. The minimum correlation value was approximately 0.2 in dekad 1 of February and April 2012 (and dekad 2 of November 2013), and the maximum correlation was approximately 0.85 in dekad 1 of January 2012. This is within the wide range of reported correlations for previous versions of TAMSAT rainfall estimates from case studies focused on Uganda, that is, 0.17–0.55 (Maidment et al. 2013) and 0.68–0.92 (Asadullah et al. 2008). Although the latter studies have been done at different spatial scales, this is still a useful indication of skill and robustness over time.

Figure 7b shows the bias and percent bias fields collated over time for wet dekads over the validation time period. On average across Africa, TAMSAT underestimates rainfall by up to 15–17 mm dekad^{-1} (black line, Fig. 7b) with a mean underestimation of approximately 4 mm dekad^{-1} (black dashed line, Fig. 7b) over the time period considered. Previous studies reported bias values from -2.78 to 3.64 mm for monthly rainfall over Uganda (Maidment et al. 2013) and 1–4 mm for monthly rainfall over the rainy seasons of 2004–06 in the Sahel (Jobard et al. 2011). As the bias and percent bias values reported here are based on dekadal (not monthly and annual) rainfall totals across all Africa (and not over a subregion), it is not unusual to observe a wider range of variability reflecting the different rainfall regimes across the continent. In terms of percentage, the spatially averaged bias over the 3 years of validation reporting is approximately -22% (gray dashed line, Fig. 7b) (min is approximately -59% in September 2012 and max is approximately 20% in February 2013). This is within the range of differences reported for point- and pixel-based rainfall estimates (see Fig. 3 in Chadwick et al. 2010; Grimes et al. 1999). It is worth noting that when compared to gauge observations interpolated through geostatistical kriging, TAMSAT does not always show a negative bias—for example, over West Africa, TAMSAT showed a small positive bias (Chadwick et al. 2010), and here positive bias is observed for January–March 2012 and February–March 2013 (Fig. 7c).

Figure 7c shows RMSD and NRMSD collated over the validation time period. Average RMSD is approximately 22 mm dekad^{-1} (black dashed line, Fig. 7c). In terms of percentage, average NRMSD is approximately 10% (gray dashed line, Fig. 7c). Although RMSD does not indicate the direction of the deviations, it quantifies the magnitude of estimation error, providing a useful measure of overall accuracy. Thus, on average the TAMSAT estimates are within 22 mm dekad^{-1} of the gauge observations, and this represents an average normalized estimation error (NRMSD) of approximately 10% relative to the observed rainfall. As discussed previously, this is in part due to the point-to-pixel mismatch. NRMSD shows less variability than RMSD over the time period considered as it removes the influence of dry dekads. It is worth noting that according to Fig. 7, there are no apparent seasonal biases present in the statistical measures used for the routine evaluation of the dekadal TAMSAT rainfall estimates.

Figure 8 shows the binary statistics and skill scores collated over the validation time period and calculated on the basis of the contingency tables of wet and dry collocated TAMSAT pixels and gauges. Average POD and BIAS are approximately 0.8 and 0.97, respectively. POD indicates that for a given dekad for approximately 80% of the locations, a dekad is correctly detected as wet
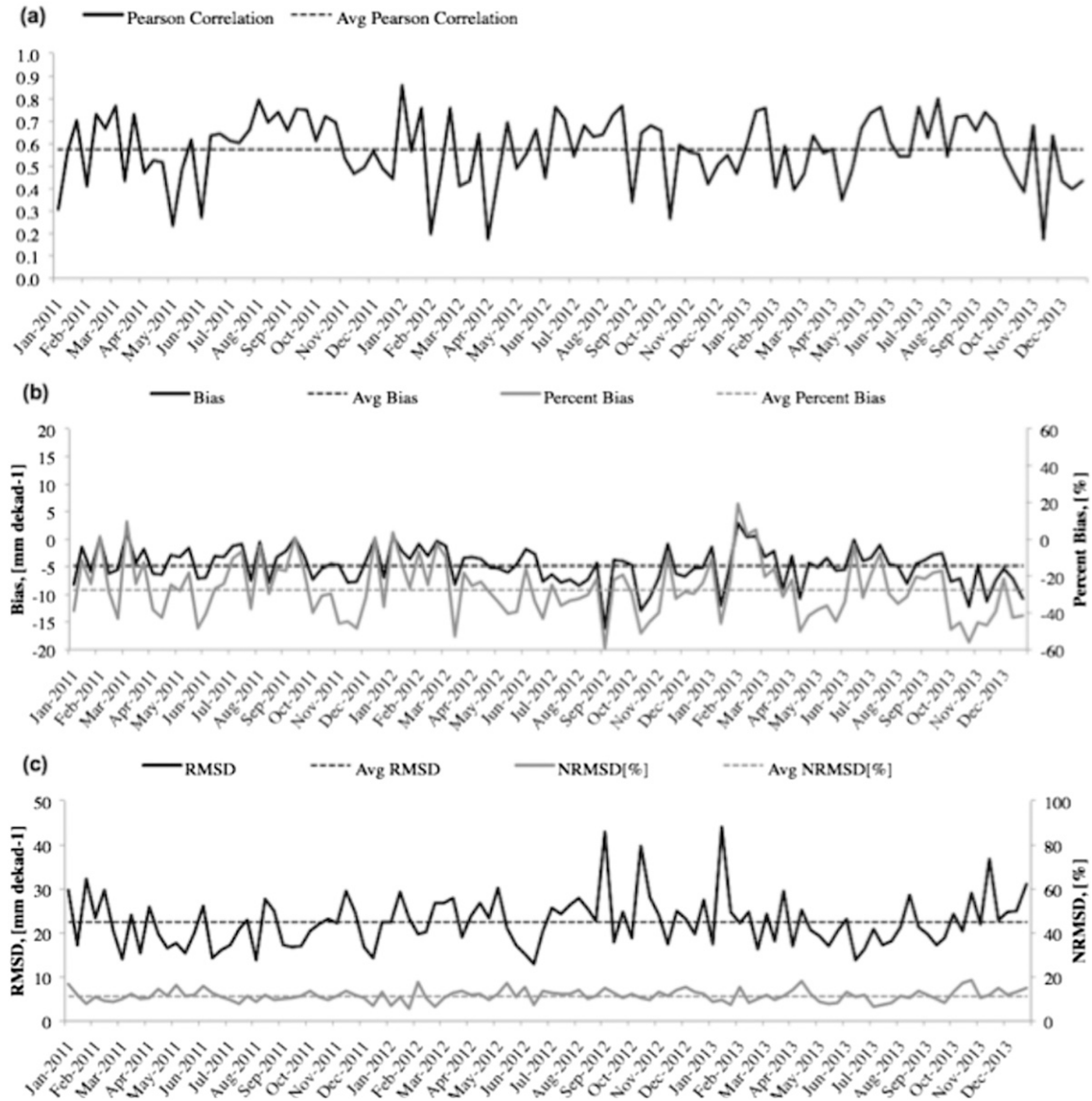
FIG. 7. (a) Pearson correlation coefficient, (b) bias (difference between the TAMSAT rainfall estimate minus gauge observation) and percent bias (percent error), and (c) RMSD and NRMSD collated over time for the 108 dekads of the validation time period from January 2011 to December 2013. Note that for each dekad, values are calculated as an average of all reported gauge observations over Africa and only for locations that are wet in the collocated TAMSAT pixels and gauges.

in the TAMSAT pixel estimates and the collocated gauge locations. For dekads when BIAS > 1 (e.g., January 2012 and November 2012 and 2013), the rainfall estimation model exhibits overestimation of wet dekads/locations, while when BIAS < 1 (e.g., July 2011 and May 2013), there is underestimation of wet dekads/locations. The FAR metric is low at approximately 0.2 (Fig. 8). On average, both HSS and HKSS are approximately 0.6 over the time period considered, indicating good skill of discrimination between wet and dry dekads/locations. The ETS score is on average approximately 0.45 and never

below zero, meaning that the TAMSAT rainfall estimation model is never unskilled.

It is worth noting that for other datasets, unlike for TAMSAT, it might not be possible to isolate the effects of varying gauge data input for such an independent comparison, yet the timely and routine delivery of information on validation metrics is one of the fundamental requirements for operational drought monitoring. Based on the results discussed here, in the next section, we reflect on the role of TAMSAT as a complementary dataset.
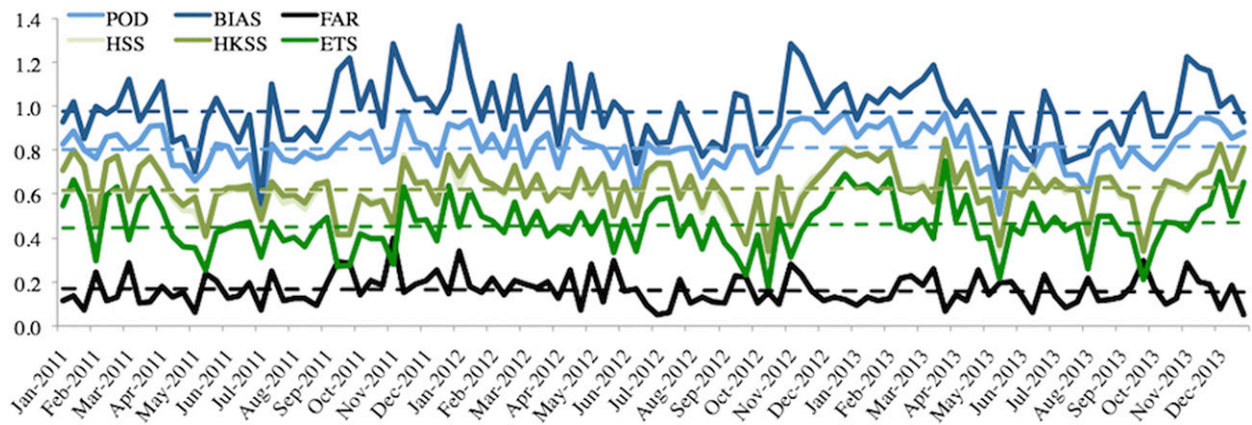
FIG. 8. POD, BIAS, FAR, HSS, HKSS, and ETS metrics for collocated TAMSAT pixels and gauge locations in each dekad collated over time for the 108 dekads of the validation time period from January 2011 to December 2013. Note that for each dekad, values are calculated as an average of all reported gauge observations over Africa and where the gauge and pixel values are >1 mm dekad^{-1}.

4. Discussion of results and applications: TAMSAT as a complementary approach for pan-African rainfall estimation

The study of Dugdale et al. (1991) over the Sahel showed that rain gauge observations alone fail to represent the spatial structure of rainfall accurately. This highlights a fundamental difference between gauge observations (point based; poorly represent the spatial structure of rainfall) and satellite rainfall estimates (pixel based; limited to the spatial resolution, at which they capture rainfall variability). The need for spatially contiguous data has motivated the development of several long-term satellite-based rainfall products issued operationally (Table 3). These products are, in some cases, designed specifically for Africa, for example, the National Oceanic Administration Climate Prediction Center (NOAA-CPC) African Rainfall Climatology (ARC) dataset (Novella and Thiaw 2013). Other products provide global coverage, for example, the GPI (Arkin and Meisner 1987), GPCP (Adler et al. 2003; Huffman et al. 1997), and the Climate Hazards Group Infrared Precipitation with Station (CHIRPS) dataset (Funk et al. 2014) released in May 2014 (Table 3). GPI data are only available monthly as the method works well for larger time periods and over large areas where

over- and underestimation of spatial and temporal errors cancel out (Hsu et al. 1997; Arkin and Meisner 1987). Both GPI and GPCP are at too coarse spatial resolution at 2.5° for operational monitoring of regional and local drought across Africa. The only comparable datasets to TAMSAT in terms of data period and resolution are ARC and CHIRPS.

Unlike TAMSAT, ARC and CHIRPS merge gauge data in real and near–real time, respectively. This means that where gauge coverage is good, these datasets can provide information on extreme rainfall on an event basis. On the other hand, TAMSAT estimates are not affected by inconsistent gauge data input, which means that the method is capable of placing rainfall variability in the context of a long-term climatology. In addition, ARC and CHIRPS use the 3-h GPI, while TAMSAT uses the 15-min (30 min prior to June 2006) Meteosat TIR imagery in order to capture short-duration convective storms. The TAMSAT rainfall estimates are thus suited for detecting unusually wet or dry conditions, and hence for triggering early warning.

Early warning and end-of-season assessment reports based on TAMSAT rainfall data are practically used in deciding food security interventions by international organizations such as United Nations agencies, including

TABLE 3. Satellite-based rainfall datasets covering 30+ years and issued operationally over Africa.

Dataset	Spatial extent	Temporal extent	Data input	Spatial resolution	Temporal resolution
GPI	40°N–40°S	1986–present	TIR	2.5°	Monthly
GPCP	Global	1979–present	TIR, PMW, gauge	2.5°	Pentad, monthly
NOAA-CPC ARC	40°N–40°S 20°W–55°E	1983–present	TIR, gauge	0.1°	Daily
CHIRPS	50°N–50°S	1981–near present	TIR, gauge	0.05°	Pentad
TAMSAT	Africa	1983–present	TIR, gauge	0.0375°	Dekadal

the Food and Agriculture Organization (FAO), World Food Program (WFP), and the United Nations Children's Fund (UNICEF), as well as regional clusters such as the Food Security and Nutrition Working Group (FSNWG) based in Nairobi (see online at http://www.disasterriskreduction.net). For example, the EC JRC uses the TAMSAT rainfall products in their Africa-wide monitoring system to assess crop growth and the drought risk that may affect pasture conditions. In support of an FAO-led livestock and market assessment mission in Uganda, TAMSAT rainfall estimates and anomalies provided supporting evidence of good to very good pasture conditions (FAO/GIEWS 2014). Some of the EC JRC reports are available publicly (e.g., Vancutsem et al. 2012). A recent ad hoc case study, for instance, showed that the dekadal TAMSAT rainfall estimates and anomalies proved more accurate than other products of similar temporal and spatial resolutions that are available in West Africa and southern Africa. This was particularly evident in the case of the drought that hit Angola and Namibia in 2012/13 (Rembold et al. 2013; Hooker et al. 2013). Specifically, the long-term coverage and temporal consistency of the new TAMSAT African rainfall product made it possible for the JRC to demonstrate to decision makers that the 2012/13 rainy season in Namibia was the second driest in the last 25 years (Hooker et al. 2013) and UNICEF referred to the JRC report on Namibia to decide in which regions they need to concentrate their interventions (see online at http://www.unicef.org/appeals/files/UNICEF_Namibia_Drought_SitRep2_22Aug2013.pdf).

Other applications of the African TAMSAT rainfall estimates include weather index-based insurance projects, identification of drought- and flood-prone regions, and monitoring the progression of the West African monsoon season. Specifically, Kucera et al. (2013) used the 2011 TAMSAT rainfall anomaly for March–May to show areas in East Africa that were prone to drought and in South Africa that were prone to flooding during this period. Additionally, the 2011 TAMSAT rainfall anomaly for June–August documented regionally the delay of the West African monsoon, prevalent dry conditions across the Sahel, and flooding due to above-average rainfall along the Guinea coast (Boyd et al. 2013).

The TAMSAT method is simple and not computationally intensive; it requires satellite data retrievals, but does not require a sophisticated operational system capable of dealing with latency in gauge reporting and the quality control of real-time gauge data. The simplicity of the operational method has enabled local meteorological services in Africa to develop their own TAMSAT systems, following training provided during calibration workshops. Local TAMSAT-based rainfall estimates are derived operationally, for example, for seasonal agrometeorological monitoring by the Sudan Meteorological Authority (SMA) using dense, locally available gauge data. On the basis of these data, seasonal agrometeorological bulletins are routinely produced by SMA from June to September each year and disseminated more widely via TAMSAT's website.

The range of applications illustrates the utility of TAMSAT's simple approach for rainfall estimation, as well as the value of its temporal consistency and long time series. This is not to say, however, that TAMSAT (or any other dataset) is universally the best choice. Advanced approaches using passive microwave (PMW), visible, and/or radar data (instead of or in addition to TIR input) for rainfall estimation have yielded reliable products, capable of providing near-real-time warning, for example, of intense rainfall events. A notable example is the NOAA Rainfall Estimate (Herman et al. 1997) that is part of the Famine Early Warning System Network (FEWSNET). Other products make use of sophisticated algorithms and new sensors to provide accurate estimates of rainfall intensity—some on sub-daily time scales. Such data include the Tropical Rainfall Measuring Mission (TRMM) Multisatellite Precipitation Analysis 3B42 (TMPA) (Huffman et al. 2007) and TRMM 3B43 products (Kummerow et al. 2000), Precipitation Estimation from Remote Sensing Information using Artificial Neural Network (PERSIANN) (Hsu and Sorooshian 2008), CPC Merged Analysis of Precipitation (CMAP) (Xie and Arkin 1997), Estimation of Precipitation by Satellite, second generation (EPSAT-SG) (Bergès et al. 2010), Rain Estimation using Forward-Adjusted Advection of Microwave Estimates (REFAME) (Behrangi et al. 2010), CPC morphing technique (CMORPH) (Joyce et al. 2004), and Kalman filter CMORPH (KF-CMORPH) (Joyce and Xie 2011), among others. However, unlike TAMSAT, CHIRPS, and ARC, these data do not cover a long enough time period for robust assessment of climate-related risk, and some of these products are, moreover, not pan-African.

In summary, the appropriate choice of product is critical to the success of operational applications. This requires careful assessment of skill through a range of standard statistical and application-specific metrics, along with consideration of the limitations and advantages of the methodological approach used. The above discussion has highlighted some of the rainfall datasets available for operational applications in Africa and has summarized the factors that suit individual datasets to particular applications. The examples given of successful applications of TAMSAT serve to illustrate its place within this constellation of products.

5. Conclusions

We described an updated climatology-based calibration approach that constitutes the TAMSAT operational system for pan-African rainfall monitoring (see the appendix), which makes use of a 28-yr archive (1983–2010) of harmonized rain gauge data from multiple sources and a quality-controlled TIR imagery. The climatology-based calibrations use more years and a greater mixture of wet and dry years than was previously achievable. The availability of considerably more gauge data has enabled the definition of a new set of homogeneous (in rainfall climatology terms) regions at finer spatial scale than was previously achievable with the more limited and sparse rain gauge datasets. The updated operational calibrations presented here were used in the development of the internally consistent 30-yr TARCAT dataset. This helps to extend the application of the TAMSAT rainfall estimates to drought monitoring for famine early warning in more regions than previously feasible and to put these estimates in the context of long-term rainfall climatology.

We presented a new methodology for consistent and routine validation of the dekadal TAMSAT rainfall estimates in near–real time and within the context of drought monitoring, including the reporting of validation results to the user community. Consistent, to an extent, with previous validations, TAMSAT showed an underestimation (negative) bias and good performance in dry–wet dekad and location detections across Africa as evaluated through binary performance measures (probability of detection, ratio bias, and false-alarm ratio) and three commonly used skill scores (Heidke skill score, Hanssen–Kuipers skill score, and equitable threat score).

Our validations confirm that different environments are not equally suited for CCD-based rainfall estimation and that spatial continuity can be an issue in some data-sparse regions. In this respect, the systematic routine evaluations presented here can help to define more precisely the limits of the CCD-based algorithm by identifying regions where further improvements in the calibration may be useful, provided that new gauge data become available in the future. Thus, future work will aim to (i) establish the relative importance of precipitation type (convective or frontal/cirrus clouds) in different regions and seasons; (ii) improve the rainfall estimation model to better relate cold cloud duration to rainfall from different storm types, evaluating the relevance of using calibration regions; and (iii) quantify the uncertainty of near-real-time rainfall estimates through validation case studies using independent gauge datasets. Finally, we gave an overview of applications, which demonstrate TAMSAT's complementary role in robust systems of early warning, climate risk management, and decision making in food security contexts.

APPENDIX

Operational TAMSAT Rainfall Estimates and Derived Products

As part of the TAMSAT rainfall monitoring system, dekadal rainfall estimates become available within a maximum of 48 h from the end of a dekad where dekad 1 products are produced on the eleventh of the month, dekad 2 products are produced on the twenty-first, and dekad 3 products are produced on the first day of the following month. At the end of each month, a monthly rainfall estimate is produced as the sum of the three dekads' rainfall estimates. To facilitate a comparison of the TAMSAT rainfall estimates with numerical weather prediction (NWP) model outputs, seasonal rainfall totals are produced as follows: December–February (DJF), March–May (MAM), June–August (JJA), and September–November (SON). Additionally, 30-yr rainfall climatologies are produced over the time period from 1983 to 2012 and dekadal, monthly, and seasonal anomalies are calculated against the respective climatology product. The TAMSAT rainfall estimates and derived products are routinely made available through TAMSAT's website and (with the exception of seasonal rainfall totals and anomalies) in near–real time via the GEONETCast data broadcasting service of EUMETSAT.

TAMSAT also issues rainfall tercile estimates operationally for verification of seasonal forecast model outputs. Seasonal forecasts of rainfall over Africa (both dynamical and statistical), such as those issued by the Met Office (UKMO), are commonly disseminated to users in the form of a map of tercile probabilities. These are available from the UKMO website (www.metoffice.gov.uk/research/climate/seasonal-to-dekadal/gpc-outlooks/glob-seas-prob). The information conveyed is how likely rainfall is to be below (0–33rd percentile), above (66th–100th percentile) or near normal (33rd–66th percentile) for a particular season when compared with climatology. For an independent evaluation of tercile forecasts at the UKMO, TAMSAT estimates are compared with the 1983–2012 TAMSAT monthly climatology to produce rainfall tercile estimates, indicating whether rainfall has been estimated to be below-, near-, or above-normal rainfall for each month and location. These estimates are available from the TAMSAT website and in the monitoring section of the Climate Science Research Partnership website (www.metoffice.gov.uk/csrp/results-products/monitoring). They are used for evaluation of seasonal forecasts over Africa by the UKMO and their partners in African NMAs. At present, the seasonal forecast evaluations are carried out internally and in a qualitative manner, and there are plans at the UKMO to undertake a routine quantitative evaluation in the future.

REFERENCES

Adler, R. F., and Coauthors, 2003: The version-2 Global Precipitation Climatology Project (GPCP) Monthly Precipitation Analysis (1979-present). *J. Hydrometeor.,* **4,** 1147–1167, doi:10.1175/1525-7541(2003)004<1147:TVGPCP>2.0.CO;2.

Arkin, P. A., 1979: The relationship between fractional coverage of high cloud and rainfall accumulations during GATE over the B-scale array. *Mon. Wea. Rev.,* **107,** 1382–1387, doi:10.1175/1520-0493(1979)107<1382:TRBFCO>2.0.CO;2.

——, and B. N. Meisner, 1987: The relationship between large-scale convective rainfall and cold cloud over the Western Hemisphere during 1982–84. *Mon. Wea. Rev.,* **115,** 51–74, doi:10.1175/1520-0493(1987)115<0051:TRBLSC>2.0.CO;2.

Asadullah, A., N. McIntyre, and M. Kigobe, 2008: Evaluation of five satellite products for estimation of rainfall over Uganda. *Hydrol. Sci. J.,* **53,** 1137–1150, doi:10.1623/hysj.53.6.1137.

Behrangi, A., K. Hsu, B. Imam, S. Sorooshian, G. J. Huffman, and R. J. Kuligowski, 2009: PERSIANN-MSA: A precipitation estimation method from satellite-based multispectral analysis. *J. Hydrometeor.,* **10,** 1414–1429, doi:10.1175/2009JHM1139.1.

——, B. Imam, K. Hsu, S. Sorooshian, T. J. Bellerby, and G. J. Huffman, 2010: REFAME: Rain estimation using forward-adjusted advection of microwave estimates. *J. Hydrometeor.,* **11,** 1305–1321, doi:10.1175/2010JHM1248.1.

Bergès, J. C., I. Jobard, F. Chopin, and R. Roca, 2010: EPSAT-SG: A satellite method for precipitation estimation; its concepts and implementation for the AMMA experiment. *Ann. Geophys.,* **28,** 289–308, doi:10.5194/angeo-28-289-2010.

Boyd, E., R. J. Cornforth, P. J. Lamb, A. Tarhule, M. Issa Lele, and A. Brouder, 2013: Building resilience to face recurring environmental crisis in African Sahel. *Nat. Climate Change,* **3,** 631–637, doi:10.1038/nclimate1856.

Chadwick, R., D. Grimes, R. Saunders, P. Francis, and T. Blackmore, 2010: The TAMORA algorithm: Satellite rainfall estimates over West Africa using multi-spectral SEVIRI data. *Adv. Geosci.,* **25,** 3–9, doi:10.5194/adgeo-25-3-2010.

Challinor, A. J., J. M. Slingo, T. R. Wheeler, P. Q. Craufurd, and D. I. F. Grimes, 2003: Toward a combined seasonal weather and crop productivity forecasting system: Determination of the working spatial scale. *J. Appl. Meteor.,* **42,** 175–192, doi:10.1175/1520-0450(2003)042<0175:TACSWA>2.0.CO;2.

Dinku, T., P. Ceccato, E. Grover-Kopec, M. Lemma, S. J. Connor, and C. F. Ropelewski, 2007: Validation of satellite rainfall products over East Africa's complex topography. *Int. J. Remote Sens.,* **28,** 1503–1526, doi:10.1080/01431160600954688.

Dugdale, G., V. McDougall, and J. Milford, 1991: Rainfall estimates in the Sahel from cold cloud statistics: Accuracy and limitations of operational systems. *Soil Water Balance in the Sudano-Sahelian Zone, Proceedings of a Workshop Held at Niamey (Niger), February 1991,* M. V. K. Sivakumar et al., Eds., IAHS Publ., **199,** 65–74.

Dybkjær, G., 2003: A simple self-calibrating cold cloud duration technique applied in West Africa and Bangladesh. *Dan. J. Geogr.,* **103,** 83–98, doi:10.1080/00167223.2003.10649482.

FAO/GIEWS, 2014: FAO/GIEWS livestock and market assessment mission to Karamoja Region, Uganda. FAO Special Rep., 32 pp. [Available online at www.fao.org/docrep/019/I3674e/I3674e.pdf.]

Flitcroft, I. D., J. R. Milford, and G. Dugdale, 1989: Relating point to area average rainfall in semiarid West Africa and the implications for rainfall estimates derived from satellite data. *J. Appl. Meteor.,* **28,** 252–266, doi:10.1175/1520-0450(1989)028<0252:RPTAAR>2.0.CO;2.

Funk, C. C., and Coauthors, 2014: A quasi-global precipitation time series for drought monitoring. U.S. Geological Survey Data Series 832, 4 pp., doi:10.3133/ds832.

Grimes, D. I. F., E. Pardo-Igúzquiza, and R. Bonifacio, 1999: Optimal areal rainfall estimation using raingauges and satellite data. *J. Hydrol.,* **222,** 93–108, doi:10.1016/S0022-1694(99)00092-X.

Herman, A., V. B. B. Kumar, P. A. Arkin, and J. V. Kousky, 1997: Objectively determined 10-day African rainfall estimates created for famine early warning systems. *Int. J. Remote Sens.,* **18,** 2147–2159, doi:10.1080/014311697217800.

Hooker, J., F. Kayitakire, F. Urbano, F. Rembold, and H. Kerdiles, 2013: Seasonal monitoring in Namibia, 2012/2013—Severe drought over the north and centre of the country. JRC Scientific and Policy Rep., 8 pp. [Available online at http://ies.jrc.ec.europa.eu/uploads/fileadmin/2013/20130814-Namibia_report_July_2013.pdf.]

Hsu, K., and S. Sorooshian, 2008: Satellite-based precipitation measurement using PERSIANN system. *Hydrological Modelling and the Water Cycle,* Vol. 63, S. Sorooshian et al., Eds., Springer, 27–48.

——, X. Gao, S. Sorooshian, and H. V. Gupta, 1997: Precipitation Estimation from Remotely Sensed Information Using Artificial Neural Networks. *J. Appl. Meteor.,* **36,** 1176–1190, doi:10.1175/1520-0450(1997)036<1176:PEFRSI>2.0.CO;2.

Huffman, G. J., and Coauthors, 1997: The Global Precipitation Climatology Project (GPCP) combined precipitation

dataset. *Bull. Amer. Meteor. Soc.,* **78,** 5–20, doi:10.1175/1520-0477(1997)078<0005:TGPCPG>2.0.CO;2.

——, and Coauthors, 2007: The TRMM Multisatellite Precipitation Analysis (TMPA): Quasi-global, multiyear, combined-sensor precipitation estimates at fine scales. *J. Hydrometeor.,* **8,** 38–55, doi:10.1175/JHM560.1.

Jobard, I., F. Chopin, J. Berges, and R. Roca, 2011: An intercomparison of 10-day satellite precipitation products during West African monsoon. *Int. J. Remote Sens.,* **32,** 2353–2376, doi:10.1080/01431161003698286.

Joyce, R. J., and P. Xie, 2011: Kalman filter–based CMORPH. *J. Hydrometeor.,* **12,** 1547–1563, doi:10.1175/JHM-D-11-022.1.

——, J. E. Janowiack, P. A. Arkin, and P. Xie, 2004: CMORPH: A method that produces global precipitation estimates from passive microwave and infrared data at high spatial and temporal resolution. *J. Hydrometeor.,* **5,** 487–503, doi:10.1175/1525-7541(2004)005<0487:CAMTPG>2.0.CO;2.

Kucera, P. A., E. E. Ebert, F. J. Turk, V. Levizzani, D. Kirschbaum, F. J. Tapiador, A. Loew, and M. Borsche, 2013: Precipitation from space: Advancing Earth system science. *Bull. Amer. Meteor. Soc.,* **94,** 365–375, doi:10.1175/BAMS-D-11-00171.1.

Kummerow, C., and Coauthors, 2000: The status of the Tropical Rainfall Measuring Mission (TRMM) after two years in orbit. *J. Appl. Meteor.,* **39,** 1965–1982, doi:10.1175/1520-0450(2001)040<1965:TSOTTR>2.0.CO;2.

Laurent, H., I. Jobard, and A. Toma, 1998: Validation of satellite and ground-based estimates of precipitation over the Sahel. *Atmos. Res.,* **47-48,** 651–670, doi:10.1016/S0169-8095(98)00051-9.

Maidment, R. I., D. I. F. Grimes, R. P. Allan, H. Greatrex, O. Rojas, and O. Leo, 2013: Evaluation of satellite-based and model re-analysis rainfall estimates for Uganda. *Meteor. Appl.,* **20,** 308–317, doi:10.1002/met.1283.

——, ——, ——, E. Tarnavsky, M. Stringer, T. Hewison, R. Roebeling, and E. Black, 2014: The 30-year TAMSAT African Rainfall Climatology and Time-Series (TARCAT) dataset. *J. Geophys. Res. Atmos.,* **119,** 10 619–10 644, doi:10.1002/2014JD021927.

Milford, J. R., and G. Dugdale, 1984: Short period forecasts in West Africa using Meteosat data. *Nowcasting-II Symp.,* Norrköping, Sweden, ESA, 255–259.

——, V. D. McDougall, and G. Dugdale, 1994: Rainfall estimation from cold cloud duration, experience of the TAMSAT group in West Africa. *Validation des Methodes D'estimation des Precipitations par Satellite,* IRD, 13–29. [Available online at http://horizon.documentation.ird.fr/exl-doc/pleins_textes/pleins_textes_6/colloques2/010008087.pdf.]

Novella, N. S., and W. M. Thiaw, 2013: African Rainfall Climatology version 2 for famine early warning systems. *J. Appl. Meteor. Climatol.,* **52,** 588–606, doi:10.1175/JAMC-D-11-0238.1.

Rembold, F., F. Urbano, H. Kerdiles, and F. Kayitakire, 2013: Seasonal monitoring in Angola ad hoc report—Southern regions of the country hit by drought, in some areas for second consecutive year. JRC Scientific and Policy Rep. MARS. Bull., 12 pp. [Available online at http://ies.jrc.ec.europa.eu/uploads/fileadmin/2013/JRC_Seasonal_monitoring_%20Angola_June2013.pdf.]

Richards, F., and P. Arkin, 1981: On the relationship between satellite-observed cloud cover and precipitation. *Mon. Wea. Rev.,* **109,** 1081–1093, doi:10.1175/1520-0493(1981)109<1081:OTRBSO>2.0.CO;2.

Snijders, F. J., 1991: Rainfall monitoring based on Meteosat data—A comparison of techniques applied to the western Sahel. *Int. J. Remote Sens.,* **12,** 1331–1347, doi:10.1080/01431169108929729.

Teo, C.-K., 2006: Application of satellite-based rainfall estimates to crop yield forecasting in Africa. Ph.D. thesis, University of Reading, 242 pp.

Thorne, V., P. Coakeley, D. Grimes, and G. Dugdale, 2001: Comparison of TAMSAT and CPC rainfall estimates with raingauges, for southern Africa. *Int. J. Remote Sens.,* **22,** 1951–1974, doi:10.1080/01431160118816.

Todd, M. C., E. C. Barrett, M. J. Beaumont, and J. L. Green, 1995: Satellite identification of rain days over the upper Nile River basin using an optimum infrared rain/no-rain threshold temperature model. *J. Appl. Meteor.,* **34,** 2600–2611, doi:10.1175/1520-0450(1995)034<2600:SIORDO>2.0.CO;2.

——, ——, ——, and T. J. Bellerby, 1999: Estimation of daily rainfall over the upper Nile river basin using a continuously calibrated satellite infrared technique. *Meteor. Appl.,* **6,** 201–210, doi:10.1017/S1350482799001206.

Tucker, M. R., and C. B. Sear, 2001: A comparison of Meteosat rainfall estimation techniques in Kenya. *Meteor. Appl.,* **8,** 107–117, doi:10.1017/S1350482701001098.

Vancutsem, C., E. Marinho, G. Pini, T. Nkunzimana, A.-C. Thomas, F. Kayitakire, F. Urbano, and M. Meroni, 2012: Bulletin sur la sécurite alimentaire Bande sahélienne de l'Afrique de l'Ouest. Conditions de la végétation par rapport à la moyenne historique (1999-2011). Situation de Mai-Julliet 2012 [Report on food security in the Sahel band in West Africa: Vegetation conditions relative to the historical average (1999-2011)—Situation as of May–July 2012]. European Commission Publ., 11 pp. [Available online at http://mars.jrc.ec.europa.eu/mars/content/download/2801/14282/file/MARS_FoodSecurityBulletin_WestAfrica_July2012.pdf.]

Xie, P., and P. A. Arkin, 1997: Global precipitation: A 17-year monthly analysis based on gauge observations, satellite estimates, and numerical model outputs. *Bull. Amer. Meteor. Soc.,* **78,** 2539–2558, doi:10.1175/1520-0477(1997)078<2539:GPAYMA>2.0.CO;2.